

# Embedding Adaptation is Still Needed for Few-Shot Learning

Sébastien M. R. Arnold  
University of Southern California  
seb.arnold@usc.edu

Fei Sha  
Google AI  
fsha@google.com

## Abstract

*Constructing new and more challenging tasks is a fruitful methodology to analyse and understand few-shot classification methods. Unfortunately, existing approaches to building those tasks are somewhat unsatisfactory: they either assume train and test task distributions to be identical — which leads to overly optimistic evaluations — or take a “worst-case” philosophy — which typically requires additional human labor such as obtaining semantic class relationships. We propose ATG, a principled clustering method to defining train and test tasks without additional human knowledge. ATG models train and test task distributions while requiring them to share a predefined amount of information. We empirically demonstrate the effectiveness of ATG in generating tasks that are easier, in-between, or harder than existing benchmarks, including those that rely on semantic information. Finally, we leverage our generated tasks to shed a new light on few-shot classification: gradient-based methods — previously believed to underperform — can outperform metric-based ones when transfer is most challenging.*

## 1. Introduction

Few-shot learning, the ability to learn from limited supervision, is essential for the real-world deployment of adaptive machines. Although proposed more than 20 years ago [37, 15], this field has recently been the focus of vast research efforts and a plethora of methods were proposed to tackle many of its challenges, including knowledge transfer and adaptation.

However, the fundamental problem of *evaluating* those methods remains largely unaddressed. Although many standardized benchmarks exist, they follow one of two recipes to generate classification tasks – they either partition classes at random (e.g. [7, 71]) or leverage class semantic relationships (e.g. [42, 53, 68]). The former implicitly assumes that train and test tasks come from the same distribution, leading to overly optimistic evaluation. The latter, although more realistic, requires additional human knowledge which can

Table 1: 5-ways 5-shots classification accuracy of metric- and gradient-based methods when transfer is most challenging. In this regime, methods that adapt their embedding function (Finetune, MAML) outperforms those that do not, and which were thought to be sufficient for few-shot learning.

	CIFAR100	mini-IN	tiered-IN	LFW10	EMNIST
ANIL	49.27%	54.42%	73.24%	77.86%	86.54%
ProtoNet	50.46%	60.36%	78.64%	85.48%	89.81%
Multiclass	53.02%	61.86%	81.90%	82.26%	90.96%
MAML	55.73%	62.25%	n/a	<b>86.36%</b>	91.92%
Finetune	<b>70.98%</b>	<b>70.47%</b>	<b>83.57%</b>	83.35%	<b>93.51%</b>

be expensive to gather, when available at all. This status quo is unsatisfactory because different applications call for different benchmarking schemes: a model that performs best when train and test tasks are similar does not necessarily achieve top accuracy when the two tasks significantly differ. In other words, the quality of a few-shot learning algorithm depends on both train and test tasks, and *their relative similarity*.

Without more fine-grained benchmarks, we might miss important properties of our algorithms and hinder their deployment to real-world scenarios. For example, recent work suggests that simply learning a good feature extractor might be *all we need* for few-shot classification [66, 49]. Notably, they match and often surpass the performance of gradient-based methods by sharing a feature extractor across all tasks and only adapting a final classification layer. But, it stands to reason that in the extreme case where train tasks contain no information relevant to the test ones (*i.e.* transfer is impossible), those methods will underperform those that are allowed to adapt their feature extractor. Table 1 displays results for such an instances where gradient-based methods (MAML [18]) dominate on tasks carefully designed to challenge transfer.

In this manuscript we propose *Automatic Taskset Generation* (ATG), a method to automatically generate tasks from existing datasets, with fine-grained control over the transfer difficulty between train and test tasks. (*c.f.* Figure 1) Our method can be understood as a penalized clustering objective that enforces a desired similarity between train and

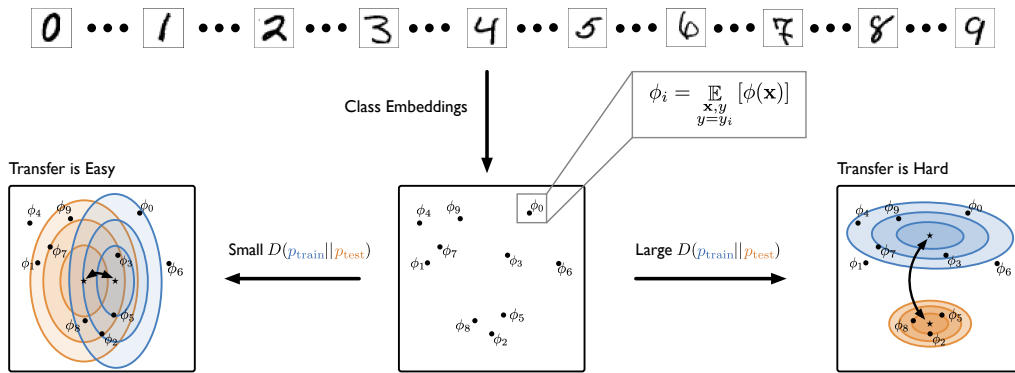


Figure 1: ATG, a method to generate tasksets of varying difficulty. First, we compute each *class embedding* by averaging the embedding  $\phi(\mathbf{x})$  of all images  $\mathbf{x}$  associated with that class. Then, we partition those class embeddings using a penalized clustering objective. If we want easy tasksets, we find clusters such that train and test classes are pulled together; for hard tasksets, we push those distributions apart.

test tasks. Importantly, it does not require additional human knowledge and is thus amenable to settings where this information is not available. We use ATG to study and evaluate the two main families of few-shot classification algorithms: gradient-based and metric-based methods. Our results on 5 tasksets, including two new ones, show that gradient-based method become particularly compelling when transfer is most challenging.

**Contributions** We make the following contributions:

- ATG, a method to automatically generate tasksets that does not require additional human knowledge.
- Extensive validation and study of our method, showing it can effectively control the degree of transfer difficulty between train and test tasks.
- An empirical analysis of popular few-shot learning methods, suggesting that gradient-based method outperform metric-based ones in the most challenging transfer regimes.

Our implementations and tasksets are described in the Supplementary Material, and are publicly available at: <http://seba1511.net/projects/atg>

## 2. Related Works

**Few-Shot Learning** The goal of few-shot learning is to produce a model able to solve new tasks with access to only limited amounts of data [15, 37]. It is closely related to meta-learning – devising models that learn to learn [6, 60] – but with a particular emphasis on the small quantity of available data. This research direction has received a lot of interest in recent years, due to the numerous applications in natural language processing [40, 81, 78], medicine [10, 2, 47], and more [77, 8, 9, 74]. In the computer vision domain, a wide-range of approaches were proposed to tackle the few-shot image classification challenge. Those include learning fast

optimization schemes [52], weight-imprinting [48], memory-augmented neural networks [59], casting the problem as stochastic process learning [21], or going about it from a Bayesian perspective [43]. This manuscript focuses on two major families of few-shot learning algorithms which we review below; for a more exhaustive account of few-shot and meta-learning, we refer the reader to the surveys of [73] and [70].

**Gradient-Based Few-Shot Learning** The main idea behind gradient-based few-shot learning algorithms is to discover a model whose parameters can be adapted with just a few steps of gradient descent [17]. The representative algorithm of this family, MAML [18], does so by learning an initialization end-to-end while adapting all weights of the model. Due to its flexible formulation, MAML was successfully applied to vision [18], robotics [12], lifelong learning [19], and more [84]. Variations of MAML improved upon its adaptation ability, reduce its computational footprint, or both. Notable attempts to improve MAML’s performance include meta-learning parameters dedicated to optimization, implicit [32, 20] or explicit [33, 44, 5], probabilistic regularization schemes [22, 80], as well as various training refinements [3]. To reduce the burden of computing second-order derivatives induced by the MAML objective, the authors suggested omitting those derivatives altogether at the cost of decreased performance. When taking several gradient steps, one can leverage the implicit function theorem to more cheaply obtain the model updates [50]. Other options to mitigate the expense of second-order derivatives consists of conditioning the model on a latent embedding, and only updating that embedding during adaptation [56, 51, 85]. In the same vein, the authors of ANIL [49] suggest that it is sufficient to update the very last layer of neural network to reap the benefits of MAML; that is, the model learns a feature extractor shared across all tasks and simply update the linear classifier a few times for each new task.

**Metric-Based Few-Shot Learning** Similar to ANIL, metric-based methods also share a feature extractor across tasks to extract high-dimensional embedding representations. But, rather than adapting a linear classifier, they compute the distance of new instances’ embeddings to the few-shot set of reference embeddings, akin to nearest neighbour classification. Matching Networks [71], which was proposed to tackle the special case of one-shot learning, uses the (negative) cosine similarity as distance measure and relies on two different networks, one for the query and one for the reference embedding. Prototypical Networks (ProtoNet) [63] generalizes Matching Networks to the few-shot setting and measures similarity between embeddings with the Euclidean distance. Some extensions to ProtoNet centered around learning and improving a specialized distance metric for a given task, typically by solving a convex optimization problem [7, 31, 83]. Others attempted to improve the embedding representations of a task [42, 54, 79, 34]. Finally, ProtoMAML [68] combined MAML with ProtoNet such that the classification layer is initialized with the reference embedding values and the model is adapted for a few steps of gradient descent.

A recent line of work put a lot of those advances in question, and show that a simple baseline matches – and often surpasses – state-of-the-art performance in few-shot classification [66, 72, 14, 11]. Rather than learning by sampling many different tasks, they suggest to aggregate the classes from all tasks and to train a model via standard one-vs-rest multiclass classification. At test time, the last linear layer of the model is removed to obtain a trained feature extractor, which can be used à la ProtoNet. Directly [66] or not, those results beg the question: *do we still need to adapt our features for few-shot learning?*

**Tasksets for Few-Shot Learning** Our manuscript tackles this question when transfer to new tasks is especially challenging. In this context, few-shot classification tasksets can be broadly categorized in two groups: those that leverage additional human information and those that don’t. In the latter case, the standard approach consists in taking an existing classification dataset and randomly partitioning classes in train and test sets. Typical examples include CIFAR-FS [7], mini-ImageNet [71, 52], TCGA [58], MultiMNIST [57, 62], CU Birds [75], FGVC Planes [36] and Fungi [64, 61], VGG Flowers [41], and Omniglot [29, 30]. Tasksets that do take advantage of human knowledge (usually in the form of semantic class relationships) attempt to minimize *information overlap* to challenge transfer. To the best of our knowledge, there are two such tasksets: FC100 [42] and tiered-ImageNet [53]. The former is built on CIFAR100 [28] and leverages its superclass structure, while tiered-Imagenet is a subset of ImageNet-1k [55] and uses the WordNet [38] database.

Building on those datasets (and some more) is Meta-

Dataset [68]: a large collection of tasksets aimed at mimicking transfer in real-world scenarios. For example, one benchmarking scenario consists of training a model on ImageNet-1k and evaluating its performance on the remaining 9 tasksets. Similar in spirit is VTAB [82], which also consists of a large collection of synthetic and natural images aimed at evaluating representation learning and transfer.

In contrast to prior work, we study the question raised by Tian *et al.* [66]: is a good embedding sufficient for few-shot learning? We approach this question from the standpoint where transfer is particularly challenging. Since training gradient-based methods on large benchmarks such as Meta-Datasets and VTAB is prohibitively expensive, we devise a method to automatically generate tasksets with explicit control over transfer difficulty.

### 3. Background and Notation

We now present the few-shot learning setting, introduce notation, and review the few-shot algorithms of interest to the remainder of this paper.

**Datasets, Tasksets, and Tasks** We designate by *dataset* a set of input-class pairs  $(\mathbf{x}, y)$ , where the dependent variable  $y$  takes values from a finite set of classes  $y_1, \dots, y_M$ . This dataset induces a classification *task*, which consists of finding a predictive function mapping  $\mathbf{x}$  to  $y$ . One common approach to construct a set of such tasks, *i.e.* a *taskset*, is to first sample a subset of  $N$  classes, and then sample  $K$  input-class pairs for each of those classes. This setting is usually referred to as  $N$ -ways  $K$ -shots.

As we often wish to evaluate the transferability of few-shot models from one taskset to another, we first partition the  $M$  classes of the dataset into train and test splits and construct tasksets from those splits. As mentioned in Section 1, partitioning can either be random, in which case train and test classes come from the same distribution, or it can leverage additional human knowledge. This additional information typically defines a hierarchy over the classes (*e.g.* semantic class relationships), which can be used for partitioning. For example, the 100 classes of CIFAR100 are grouped into 20 superclasses, and FC100 uses 12 of those superclasses (60 classes) for training and 4 (20 classes) for validation and testing, each. Once tasksets are defined, the goal of a few-shot learning algorithm is to find a model of the train tasks that generalizes to the test tasks.

To achieve this goal, we associate to each task  $\tau$  a loss  $\mathcal{L}_\tau$  and a parameterized model  $p_\tau(y | \mathbf{x})$ . Without loss of generality, we write this model as the composition of a linear layer  $w$  and a feature extractor  $\phi$  (*e.g.* a neural network). Then, finding a maximum likelihood solution for  $\phi$  and  $w$  boils down to minimizing the average task loss  $\mathbb{E}_\tau [\mathcal{L}_\tau(\phi, w)]$  over the training tasks.

**Algorithms** Gradient-based methods, and MAML in particular, compute the likelihood after adapting  $\phi$  and  $w$  for one (or a few) gradient step. For the  $i$ th class, this likelihood takes the form:

$$\begin{aligned} p_\tau(y = y_i | \mathbf{x}) &= \text{softmax}(\phi'(\mathbf{x})^\top w'_i) & (\text{MAML}) \\ \text{s.t. } w' &= w - \alpha \nabla_w \mathcal{L}_\tau \\ \phi' &= \phi - \alpha \nabla_\phi \mathcal{L}_\tau \end{aligned}$$

where  $\alpha$  denotes the adaptation learning rate, and  $w'_i$  is the  $i$ th column of the adapted linear layer. In the adaptation step, the gradient of the loss is computed over the set of few-shot examples; differentiating it requires Hessian-gradient products which makes MAML an expensive method for large feature extractor  $\phi$ . For this reason, MAML is rarely used with architectures larger than the standard 4-layer CNN. To scale up MAML to the 12-layer ResNet of our experiments, we implement a data-parallel version of MAML where different GPUs are responsible for different subsets of the few-shot inputs. Refer to the Supplementary Material for more details.

To alleviate this computational burden, the authors of ANIL suggest that adapting  $w$  is sufficient to claim many of MAML’s benefits:

$$\begin{aligned} p_\tau(y = y_i | \mathbf{x}) &= \text{softmax}(\phi(\mathbf{x})^\top w'_i) & (\text{ANIL}) \\ \text{s.t. } w' &= w - \alpha \nabla_w \mathcal{L}_\tau. \end{aligned}$$

Contrasting with MAML, the difference lies in the feature extractor  $\phi$  being shared – *not* adapted – across tasks. In that sense ANIL resembles metric-based methods, despite its original motivation of approximating MAML. Since  $\phi$  is responsible for the bulk of the computation, ANIL becomes increasingly more efficient as the feature extractor grows in size.<sup>1</sup>

A representative metric-based algorithm, ProtoNet also shares  $\phi$  across tasks and replaces the final linear classifier by a nearest neighbour one. It measures this nearest neighbour distance between the query embedding  $\phi(\mathbf{x})$  and the  $i$ th class embedding  $\phi_i$ :

$$p_\tau(y = y_i | \mathbf{x}) = \text{softmax}(-d(\phi(\mathbf{x}), \phi_i)) \quad (\text{ProtoNet})$$

where  $\phi_i = \mathbb{E}_{\mathbf{x} \sim p_\tau(\cdot | y_i)}[\phi(\mathbf{x})]$  is the average embedding of the few samples with class  $y_i$ , and  $d(\cdot, \cdot)$  is a distance function – common choices include the Euclidean norm or the (negative) cosine similarity.

Since the ProtoNet classifier is nonparametric, it can be used with any feature extractor  $\phi$ . Thus, a simple yet effective baseline, *Multiclass*, consists of collapsing all train tasks into a single large tasks and learning a feature extractor via standard one-vs-rest multiclass classification. At test-time, we can readily use this learned feature extractor with the ProtoNet classifier to solve unseen tasks.

<sup>1</sup>In our experiments, we saw speed-ups as large as 9.25x over MAML.

## 4. Taskset Generation: Easy or Hard?

This section describes ATG, a method for generating tasksets without requiring additional human knowledge, and which provides fine-grained control over the transfer difficulty between train and test tasks.

Our goal is to partition classes into train and test sets, such that we can control the difficulty of transferring a model trained on one set to the other. At a high-level, ATG finds those class partitions based on their *class embedding*  $\phi_1, \dots, \phi_M$ . Each class embedding  $\phi_i$  is obtained by averaging the embedding of all samples from its corresponding class  $y_i$ :

$$\phi_i = \mathbb{E}_{\mathbf{x} \sim p(\cdot | y_i)}[\phi(\mathbf{x})],$$

where  $\phi$  is a pretrained feature extractor. In practice, we find that pretraining  $\phi$  on the dataset to be partitioned leads to satisfying results, but simpler approaches might also work. (e.g. an off-the-shelf model pretrained on ImageNet)

The key feature of ATG is that train and test clusters are encouraged to stay at a *prespecified distance of each other* in the class embedding space. Intuitively, the farther and tighter the test set, the more difficult it will be for few-shot methods to discriminate between those classes. On the other hand, a test task is easily solved if its classes are dissimilar (*i.e.* poorly clustered) and each class is fairly similar to classes seen during training (*i.e.* train and test clusters are adjacent).

To formalize this intuition, we pretend that the class embeddings were sampled from the mixture of two distributions  $p_{\text{train}}(y)$  and  $p_{\text{test}}(y)$ . We model  $p_{\text{train}}$  and  $p_{\text{test}}$  as multinomials such that their density for class  $y_i$  depends on its distance to the distribution’s centroid:

$$\begin{aligned} p_{\text{train}}(y = y_i) &= \text{softmax}(\|\phi_i - \mu_{\text{train}}\|^2), \quad \text{and} \\ p_{\text{test}}(y = y_i) &= \text{softmax}(\|\phi_i - \mu_{\text{test}}\|^2), \end{aligned}$$

where the centroids  $\mu_{\text{train}}$  and  $\mu_{\text{test}}$  are learnable parameters. Maximizing the log-likelihood of the mixture  $\frac{1}{2}(p_{\text{train}} + p_{\text{test}})$  is identical to a soft K-means objective if  $p_{\text{train}}$  and  $p_{\text{test}}$  were Gaussians [35, Chapter 22]. In practice, we preferred multinomials because Gaussians led to numerical instabilities when optimizing the penalized objective (see below) by gradient descent.

We can incentivize  $p_{\text{train}}$  and  $p_{\text{test}}$  to lie at a given distance  $R \geq 0$  by including a penalty  $(D(p_{\text{train}} || p_{\text{test}}) - R)^2$  based on our choice of statistical divergence  $D$ . Combining this penalty with the mixture’s log-likelihood yields our final penalized clustering objective:

$$\begin{aligned} J = & - \sum_{i=0}^M \log \frac{1}{2} (p_{\text{train}}(y_i) + p_{\text{test}}(y_i)) \\ & + \lambda (D(p_{\text{train}} || p_{\text{test}}) - R)^2, \end{aligned}$$



where  $\lambda \geq 0$  balances the value of clustering versus the penalty. Assuming train and test classes tightly cluster, controlling the transfer difficulty amounts to controlling the distance  $D(p_{\text{train}}||p_{\text{test}})$  between the two distributions, which we can achieve by adjusting  $R$ .

**Train, Validation, and Test Assignments** When  $J$  is minimized with respect to  $\mu_{\text{train}}$  and  $\mu_{\text{test}}$ , we get a solution we can use to partition  $y_1, \dots, y_M$ . One approach is to assign class  $y_i$  to the train set if the ratio  $\frac{p_{\text{train}}(y_i)}{p_{\text{test}}(y_i)}$  is greater than 1, and to the test set if less.<sup>2</sup>

Partitioning according to this decision rule is theoretically sound but might lead to slightly degenerate solutions in the context of few-shot learning. For example, we observed instances where only 3 classes were assigned to the test set, which prevents evaluation in the 5-ways setting. It also doesn't prescribe how to devise a validation set from the test distribution. To resolve those issues, we select the top 60% scoring classes and assign them to the train set. The remaining 40% classes are split among validation and test sets in turn, according to their score: the least scoring class is assigned to the test set, the second-least scoring to the validation, etc... Thus, validation and test classes retain roughly equal probability under  $p_{\text{test}}$  and the resulting tasks are of similar difficulty.

## 5. Experiments

Our experiments focus on three aspects. First, we empirically validate our proposed method to control the information overlap between train and test classes. To provide an intuitive picture of our method, we also perform an ablation study on the different measures of information and visualize low-dimensional projections of the resulting partitions. Second, we compare the partitions obtained from our method to the ones obtained using semantic class relationships. Our results suggest that both types of partitions are significantly different; moreover, they confirm that our method is capable of generating partitions that are more challenging than the ones resting on semantics. Finally, we leverage our partitions to compare gradient-based and metric-based classification methods. Those experiments indicate that metric-based methods – which were recently thought to be sufficient for few-shot learning – tend to underperform in challenging transfer settings when compared to their gradient-based counterpart.

For additional experimental details, including the exact partitions for all tasksets, please see the Supplementary Material.

<sup>2</sup>Ties are broken at random, so that if  $D(p_{\text{train}}||p_{\text{test}}) = 0$  assignments are also random.

### 5.1. Setup

Our experiments build on architectures and datasets widely used in the computer vision and few-shot learning literature. We denote by CNN4 the 4-layer CNN with 64 hidden described in [63], which we use for few-shot learning experiments on FC100, CIFAR-FS, EMNIST, and LFW10. (The latter two datasets are described below.) On mini-ImageNet and tiered-ImageNet, we use the 12-layer residual network (ResNet12) described in [39], and add the Drop-Block layers proposed in [31] for regularization. (But unlike Lee *et al.* we keep the final average pooling layers.) For experiments involving Imagenet-1k – and including Birds, Planes, Flowers, Fungi – we use 3 architectures: a 121-layer DenseNet (DenseNet121; [25]), a 18-layer residual network (ResNet18; [24]), and a GoogLeNet (GoogLeNet; [65]). For all models, we define the feature extractor to be the architecture up to the last fully-connected layer.

All tasksets built with ATG follow an identical recipe. We pretrain  $\phi$  on the same data used to compute the class embeddings  $\phi_i$ . We minimize  $J$  by gradient descent with  $\lambda = 1$ , and, unless specified otherwise, use the symmetrized version of the KL divergence for  $D$ .

With this manuscript, we also contribute tasksets for two datasets previously not used in the few-shot learning setting: EMNIST and LFW10.

**EMNIST** The Extended MNIST dataset (EMNIST; [13]) is a variant of the MNIST dataset consisting of 814,255 grayscale images of 62 handwritten characters (digits, lowercase and uppercase alphabet). Each image contains a single character scaled to 28x28 pixels. Using ATG, we partition its classes in 37 characters for training, 12 for validation, and 13 for testing, filling a niche in the few-shot dataset landscape: EMNIST is lightweight (roughly 610Mb) with few training classes, but plenty of data (>10k) available per class.

**LFW10** We bootstrap LFW10 from the *Labelled Faces in the Wild* dataset [26], which contains 13,233 pictures of 5,749 famous personalities. Of those 5k personalities, we select all 158 that have at least 10 images in the dataset – fewer would constrain the few-shot learning setup – and partition them in tasksets of 94 train, 32 validation, and 32 test classes. Each image is rescaled to 62x47 pixels with RGB colors. LFW10 is an example of dataset for which collecting class relationships is difficult if not impossible, as it requires putting a semantic hierarchy over each individual in the dataset.

### 5.2. Controlling Information Overlap

We first test whether our method is effective in producing tasksets of varying difficulty. To that end, we use ATG to

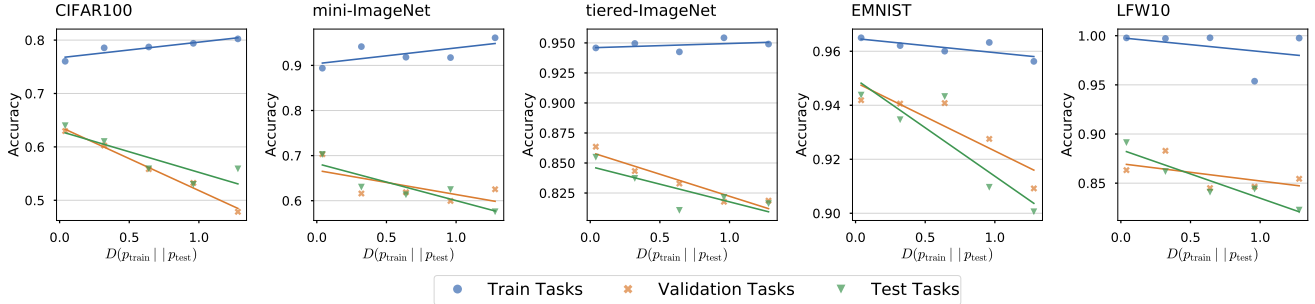


Figure 2: Accuracy of a Multiclass-trained network as we increase the divergence between train and test class distributions. As the divergence increases, accuracy drops suggesting that the divergence can be used to generate tasksets of varying difficulty.

generate tasksets of increasing difficulty on the classes of 5 datasets: CIFAR100, mini-ImageNet, tiered-ImageNet, LFW10, and EMNIST. First, we train a convolutional network over the entire set of classes, using the standard cross-entropy minimization. We use a 121-layer DenseNet for CIFAR100, mini- and tiered-ImageNet dataset, and the CNN4 for LFW10 and EMNIST. We then remove the last fully-connected layer of the network, and use this feature extractor to compute the mean embedding of each class. Finally, we create train, validation, and test class partitions for various target divergence between train and test classes.

We measure transfer difficulty with the 5-ways 5-shots classification accuracy of a model trained with Multiclass on the train taskset only. We use the ResNet12 for ImageNet-based tasks, and the CNN4 for the others. Figure 2 reports train, validation, and test accuracies as a function of the divergence for all datasets. Across all datasets test accuracy decreases as the divergence between train and test class distributions increases. Thus, we conclude that our method is effective in finding partitions of desired transfer difficulty. We also observe that validation and test accuracies similarly challenge the transfer ability of the Multiclass model, which is expected as both sets of classes come from the same distribution.

**PCA Visualizations** We perform two more ablative studies to provide further understanding of ATG. In Figure 3, we plot the 2-dimensional PCA projection of the CIFAR100 mean class embeddings, together with their assignments and the assigned centroid. We observe that centroids separate further as the divergence increases from 0.04 to 1.28 – the greater the divergence between  $p_{\text{train}}$  and  $p_{\text{test}}$ , the further  $\mu_{\text{train}}$  and  $\mu_{\text{test}}$ .

**Comparing Divergences** Although intuitive, this description is not sufficient to explain why ATG works because it lacks a measure of how difficult it is to discriminate between the classes of a task. To show this, we compare different methods for measuring the distance of train and test

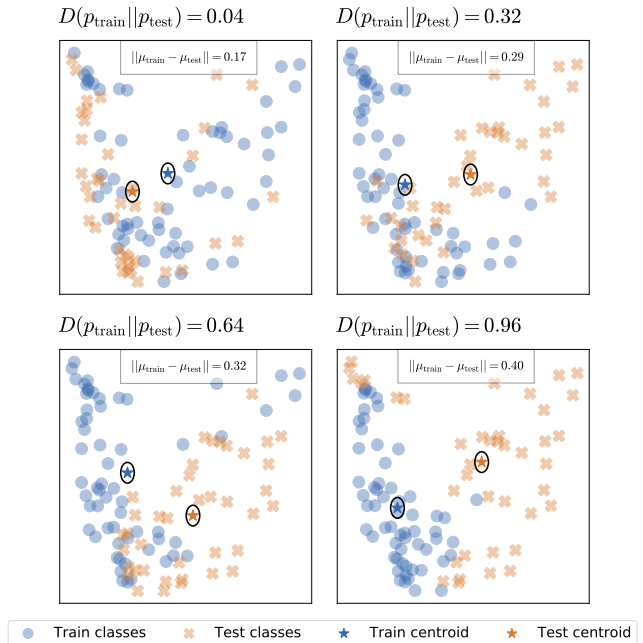


Figure 3: Low-dimensional projections of class embeddings and taskset centroids. As we increase the divergence penalty, the centroids spread further apart.

class distributions between ImageNet-1k and 4 downstream datasets. (Birds, Planes, Fungi, and Flowers) We take a 121-layer DenseNet pretrained on ImageNet-1k, and compute the mean class embedding for all 1,000 classes as well as the ImageNet centroid. Then, for each of the downstream dataset, we sample 100 tasks, each consisting of 5 classes and 5 samples. Finally, we compute the distance between the train distribution (defined by the ImageNet centroid) and the task distribution (defined by the centroid of the task) over all 1,005 classes.

Table 2 reports the Pearson’s correlation coefficient between those distance measurements and the task accuracies for all datasets. The symmetrized KL, which we use in our remaining experiments, performs best while naively measuring the Euclidean distance between centroids (Eu-

Table 2: Correlation between divergence and accuracy for different choice of divergence  $D$ . Measuring the Euclidean distance between centroids performs worst, while the symmetrized KL divergence (used in our other experiments) is best.

	Birds	Planes	Fungi	Flowers
Euclidean Distance	-0.50	-0.08	-0.17	-0.33
Wasserstein-2	-0.57	-0.24	-0.23	-0.30
Kullback-Leibler	-0.63	-0.41	<b>-0.51</b>	-0.29
Symmetrized KL	<b>-0.73</b>	<b>-0.43</b>	-0.49	<b>-0.43</b>

clidan) performs worse. As a final remark, let us observe that correlations have fairly low magnitudes, indicating that our method is ill-suited to accurately measure individual task difficulty. Assessing task similarity and difficulty is an open research question; we refer the reader to related literature [1, 16, 14, 76] for more details.

### 5.3. Comparing Semantic vs Embedding Clusters

We continue the study of our method and zero-in on the difference between class embeddings and semantic to encode class similarities.

**Comparison to WordNet** The first question we ask is whether class embeddings capture information similar to semantics. To that end, we compare hierarchies created by clustering class embeddings to WordNet, the hierarchy over ImageNet-1k classes induced by class semantics.

We construct three sets of ImageNet-1k embeddings with three different pretrained architectures. For each set, we obtain a tree of their classes via Ward clustering. To compare those trees against the WordNet graph of classes, we define the *hop* distance – the average difference of distances between two classes  $a, b$ :

$$\sum_{a,b} |d_{\text{Clustering}}(a,b) - d_{\text{WordNet}}(a,b)|,$$

where  $d_{\text{Clustering}}, d_{\text{WordNet}}$  are the normalized minimum number of nodes separating  $a$  to  $b$  in the clustering tree and WordNet graph, respectively. We use such a cumbersome metric because WordNet contains cycles as well as several vertices of degree 2; intuitively, this metric can be understood as the average difference in the number “hops” necessary to reach  $b$  starting from  $a$  between the two graphs.

Table 3 reports the hop distance between WordNet and clustering trees, when the class embeddings are computed using DenseNet121, GoogLeNet (embedding sizes 104) and ResNet18. (embedding size 512) Regardless of embedding size or network architecture, the clustering structures differ from the WordNet structure by a factor of 4, indicating that class embeddings encode attributes significantly different from class semantics.

Table 3: Average hop distance between WordNet and hierarchies created from Imagenet-1k embeddings (via hierarchical clustering). Regardless of the network architecture, trees constructed from class embeddings are more similar to each other than WordNet, indicating that class partitioning relies on attributes different from semantic relationships.

	ResNet18	DenseNet121	GoogLeNet
ResNet18	0.0	1.99	2.18
DenseNet121	1.99	0.0	2.26
GoogLeNet	2.18	2.26	0.0
WordNet	<b>8.60</b>	<b>8.35</b>	<b>8.59</b>

Anecdotally, we manually inspect the trees generated from embeddings in an attempt to shed some light on what those properties might be. We find that the mean class embeddings tended to encode visual properties. For example, the *traffic light* and *theatre* classes are clustered close-by (3 hops) due to both containing many red pixels. On the other hand, the Orangutan and Macaque classes (fairly close semantic-wise) are separated by 9 hops — likely due to the difference in color and texture of both animal’s furs.

**Comparison across Methods** Having established that ATG can generate tasksets different from those built on semantics, we answer the next natural question: *How do those tasksets compare to existing tasksets?* Accordingly, we select the easy ( $D = 0.04$ ) and hard ( $D = 0.96$ ) tasksets generated with ATG and train networks with 4 popular few-shot methods (MAML, ANIL, ProtoNet, Multiclass) on the 5-ways 1-shot and 5-ways 5-shots setting on the tasksets of CIFAR100, mini-ImageNet, and tiered-ImageNet. To ensure fair comparison, we do not augment the data and use the exact same architecture for all methods within a dataset. (CNN4 for CIFAR100, ResNet12 for mini/tiered-ImageNet.<sup>3</sup>) Each (method, taskset) pair is tuned independently, using a logarithmic-spaced grid-search. For MAML and ANIL, we measure accuracy after 5 adaptation steps.

Table 4 reports the test accuracy obtained at the best validation iteration. In almost all scenarios, ATG is able to generate tasksets that are as — or even more — challenging as the tasksets constructed from semantic relationships. This makes ATG a compelling solution to taskset generation in settings where additional inter-class information is hard or even impossible to obtain. Conversely, we see that the easier tasksets generate by our method (the ones with 0.04 divergence) are significantly easier, sometimes even approaching purely random assignments. (*i.e.* with a divergence of 0)

<sup>3</sup>Training a ResNet12 with MAML on tiered-ImageNet was *still* too computationally expensive, despite our data-parallel implementation.

Table 4: Comparing classification accuracy of different tasksets for a same dataset across popular few-shot learning methods. Our proposed method, ATG, is capable of generating simple tasksets (close to random partitioning) as well as challenging ones. In particular, it is often more challenging than tasksets built with class semantics (denoted with a †), but unlike those it does not require additional information. **Bolded** results indicate most challenging taskset for a given method.

Dataset	Tasksets	Backbone	5-ways 1-shot				5-ways 5-shots			
			MAML	ANIL	ProtoNet	Multiclass	MAML	ANIL	ProtoNet	Multiclass
CIFAR100	CIFAR-FS	CNN4	56.96%	54.47%	54.97%	54.82%	72.99%	69.44%	72.00%	68.83%
	FC100†	CNN4	36.99%	35.54%	36.25%	36.59%	<b>51.48%</b>	50.12%	51.16%	<b>51.22%</b>
	Random	CNN4	56.66%	51.43%	51.25%	52.39%	73.16%	69.81%	71.12%	69.24%
	Easy (ours)	CNN4	48.35%	46.03%	46.68%	46.92%	65.19%	59.43%	63.66%	63.97%
	Hard (ours)	CNN4	<b>35.86%</b>	<b>33.55%</b>	<b>35.59%</b>	<b>35.44%</b>	55.73%	<b>49.27%</b>	<b>50.46%</b>	53.02%
mini-ImageNet	Original	ResNet12	58.80%	55.02%	56.68%	57.12%	72.56%	64.74%	71.05%	71.88%
	Random	ResNet12	53.12%	50.34%	51.58%	51.88%	72.25%	62.77%	69.70%	72.03%
	Easy (ours)	ResNet12	53.75%	51.22%	52.25%	52.53%	67.92%	61.98%	66.64%	70.27%
	Hard (ours)	ResNet12	<b>44.87%</b>	<b>42.54%</b>	<b>41.83%</b>	<b>44.62%</b>	<b>62.25%</b>	<b>54.42%</b>	<b>60.36%</b>	<b>61.86%</b>
tiered-ImageNet	Original†	ResNet12	n/a	56.99%	<b>61.59%</b>	66.75%	n/a	74.81%	80.02%	82.53%
	Random	ResNet12	n/a	62.69%	69.35%	70.89%	n/a	80.60%	85.46%	86.98%
	Easy (ours)	ResNet12	n/a	59.53%	64.39%	68.16%	n/a	76.57%	84.33%	85.50%
	Hard (ours)	ResNet12	n/a	<b>56.19%</b>	62.91%	<b>65.48%</b>	n/a	<b>73.24%</b>	<b>78.64%</b>	<b>81.90%</b>

#### 5.4. Is a Good Embedding Really Enough?

Table 5: Slope of the regression line between divergence and accuracy (in % points) for different methods. MAML degrades at slower rate than metric-based methods, suggesting that it is better suited when transfer is challenging.

	CIFAR100	mini-ImageNet	LFW10	EMNIST
MAML	<b>-11.53</b>	<b>-6.68</b>	<b>-3.10</b>	<b>-2.55</b>
ANIL	-12.44	-7.32	-3.61	-5.70
ProtoNet	-14.88	-7.18	-4.45	-4.71
Multiclass	-12.41	-7.41	-4.91	-3.23

A closer inspection of the results in Table 4 hints at an unexpected trend: *MAML becomes increasingly more competitive as the transfer from train to test classes become more challenging*. To verify this hypothesis, we train all 4 few-shot algorithms on all tasksets of 4 datasets highlighted in Section 5.2; then, we compute the slope of the regression line between divergence and test accuracies. Table 5 reports those slopes, and confirms our hypothesis: gradient-based methods degrade slower than metric-based ones.

In turn, those experiments suggest a follow-up hypothesis: *when train-test transfer is challenging enough, methods that adapt their embedding function should outperform those that do not*. We verify this hypothesis in Table 1 where we compare accuracies of each algorithms on the most challenging taskset of each dataset. We also include a *Finetune* entry, which corresponds to Multiclass with the embedding function updated by 5 gradient steps on test tasks. Confirming our hypothesis, MAML and Finetune dominate on all datasets.

## 6. Conclusion

This manuscript focuses on the evaluation and analysis of few-shot classification methods. Accordingly, we propose ATG to generate tasksets of desired transfer difficulty, and with no requirement for additional human information about classes or their relationships. After empirically validating ATG, we generate tasksets to study the two main families of few-shot classification algorithms: gradient-based and metric-based. As opposed to recent work suggesting that a good feature extractor might be enough for few-shot classification [66, 49], we find that gradient-based methods outperform metric-based ones, especially when transfer is challenging.

Although seemingly contradicting, we believe the two hypotheses are compatible: when applied out of domain the metric implicitly learned by ProtoNet and Multiclass will likely require adaptation, *e.g.* to adjust for domain shift or to discover new features. For similar reasons and as highlighted in our experiments, ANIL’s approximation of MAML will break since it does not adapt its feature extractor to avoid expensive second-order derivatives.

On the other hand, those methods don’t have to pay the price of adaptation when knowledge transfer is sufficient to reach good performance, and can thus be scald to much larger datasets. In fact, when test tasks are similar to training, MAML’s adaptation by gradient descent can even lead to overfitting especially when working with limited labelled data.

We hope our contribution can help researchers analyse few-shot learning methods and answer some of the above questions. Future research directions for ATG include extensions to regression and multi-label classification tasks.



## **Acknowledgements**

Fei Sha is on leave from University of Southern California. This work is partially supported by NSF Awards IIS-1513966/ 1632803/1833137, CCF-1139148, DARPA Award#: FA8750-18-2-0117, DARPA-D3M - Award UCB-00009528, Google Research Awards, gifts from Facebook and Netflix, and ARO# W911NF-12-1-0241 and W911NF-15-1-0484.

## References

- [1] Alessandro Achille, Michael Lam, Rahul Tewari, Avinash Ravichandran, Subhansu Maji, Charles C Fowlkes, Stefano Soatto, and Pietro Perona. Task2vec: Task embedding for meta-learning. In *Proceedings of the IEEE International Conference on Computer Vision*, pages 6430–6439, 2019. 7
- [2] Han Altae-Tran, Bharath Ramsundar, Aneesh S Pappu, and Vijay Pande. Low data drug discovery with One-Shot learning. *ACS Cent Sci*, 3(4):283–293, Apr. 2017. 2
- [3] Antreas Antoniou, Harrison Edwards, and Amos Storkey. How to train your MAML. In *International Conference on Learning Representations*, 2019. 2
- [4] Sébastien M R Arnold, Praateek Mahajan, Debajyoti Datta, Ian Bunner, and Konstantinos Saitas Zarkias. learn2learn: A library for Meta-Learning research. Aug. 2020. 14
- [5] Harkirat Singh Behl, Atılım Güneş Baydin, and Philip H S Torr. Alpha MAML: Adaptive Model-Agnostic Meta-Learning. May 2019. 2
- [6] Y Bengio, S Bengio, and J Cloutier. Learning a synaptic learning rule. In *IJCNN-91-Seattle International Joint Conference on Neural Networks*, volume ii, pages 969 vol.2–, July 1991. 2
- [7] Luca Bertinetto, Joao F Henriques, Philip Torr, and Andrea Vedaldi. Meta-learning with differentiable closed-form solvers. Sept. 2018. 1, 3
- [8] Luca Bertinetto, João F Henriques, Jack Valmadre, P Torr, and A Vedaldi. Learning feed-forward one-shot learners. *NIPS*, 2016. 2
- [9] A Brock, T Lim, J M Ritchie, and N Weston. SMASH: One-Shot model architecture search through HyperNetworks. *ICLR*, 2018. 2
- [10] Aihua Cai, Wenxin Hu, and Jun Zheng. Few-Shot learning for medical image classification. In *Artificial Neural Networks and Machine Learning – ICANN 2020*, pages 441–452. Springer International Publishing, 2020. 2
- [11] Yinbo Chen, Xiaolong Wang, Zhuang Liu, Huijuan Xu, and Trevor Darrell. A new Meta-Baseline for Few-Shot learning. Mar. 2020. 3
- [12] Ignasi Clavera, Anusha Nagabandi, Simin Liu, Ronald S. Fearing, Pieter Abbeel, Sergey Levine, and Chelsea Finn. Learning to adapt in dynamic, real-world environments through meta-reinforcement learning. In *International Conference on Learning Representations*, 2019. 2
- [13] Gregory Cohen, Saeed Afshar, Jonathan Tapson, and Andre Van Schaik. Emnist: Extending mnist to handwritten letters. In *2017 International Joint Conference on Neural Networks (IJCNN)*, pages 2921–2926. IEEE, 2017. 5
- [14] Guneet Singh Dhillon, Pratik Chaudhari, Avinash Ravichandran, and Stefano Soatto. A baseline for few-shot image classification. In *International Conference on Learning Representations*, 2020. 3, 7
- [15] Li Fei-Fei, Rob Fergus, and Pietro Perona. One-shot learning of object categories. *IEEE Trans. Pattern Anal. Mach. Intell.*, 28(4):594–611, Apr. 2006. 1, 2
- [16] Christopher Fifty, Ehsan Amid, Zhe Zhao, Tianhe Yu, Rohan Anil, and Chelsea Finn. Measuring and harnessing transfer in Multi-Task learning. Oct. 2020. 7
- [17] Chelsea Finn. *Learning to Learn with Gradients*. PhD thesis, UC Berkeley, July 2018. 2
- [18] Chelsea Finn, Pieter Abbeel, and Sergey Levine. Model-agnostic meta-learning for fast adaptation of deep networks. volume 70 of *Proceedings of Machine Learning Research*, pages 1126–1135, International Convention Centre, Sydney, Australia, 06–11 Aug 2017. PMLR. 1, 2
- [19] Chelsea Finn, Aravind Rajeswaran, Sham Kakade, and Sergey Levine. Online meta-learning. volume 97 of *Proceedings of Machine Learning Research*, pages 1920–1930, Long Beach, California, USA, 09–15 Jun 2019. PMLR. 2
- [20] Sebastian Flennerhag, Andrei A. Rusu, Razvan Pascanu, Francesco Visin, Hujun Yin, and Raia Hadsell. Meta-learning with warped gradient descent. In *International Conference on Learning Representations*, 2020. 2
- [21] Marta Garnelo, Jonathan Schwarz, Dan Rosenbaum, Fabio Viola, Danilo J Rezende, S M Ali Eslami, and Yee Whye Teh. Neural processes. July 2018. 2
- [22] Erin Grant, Chelsea Finn, Sergey Levine, Trevor Darrell, and Thomas Griffiths. Recasting gradient-based meta-learning as hierarchical bayes. In *International Conference on Learning Representations*, 2018. 2
- [23] Charles R. Harris, K. Jarrod Millman, St’efan J. van der Walt, Ralf Gommers, Pauli Virtanen, David Cournapeau, Eric Wieser, Julian Taylor, Sebastian Berg, Nathaniel J. Smith, Robert Kern, Matti Picus, Stephan Hoyer, Marten H. van Kerkwijk, Matthew Brett, Allan Haldane, Jaime Fern’andez del R’io, Mark Wiebe, Pearu Peterson, Pierre G’erard-Marchant, Kevin Sheppard, Tyler Reddy, Warren Weckesser, Hameer Abbasi, Christoph Gohlke, and Travis E. Oliphant. Array programming with NumPy. *Nature*, 585(7825):357–362, Sept. 2020. 14
- [24] Kaiming He, Xiangyu Zhang, Shaoqing Ren, and Jian Sun. Deep residual learning for image recognition. In *Proceedings of the IEEE conference on computer vision and pattern recognition*, pages 770–778, 2016. 5
- [25] Gao Huang, Zhuang Liu, Laurens Van Der Maaten, and Kilian Q Weinberger. Densely connected convolutional networks. In *Proceedings of the IEEE conference on computer vision and pattern recognition*, pages 4700–4708, 2017. 5
- [26] Gary B Huang and Erik Learned-Miller. Labeled faces in the wild: Updates and new reporting procedures. *Dept. Comput. Sci., Univ. Massachusetts Amherst, Amherst, MA, USA, Tech. Rep.*, pages 14–003, 2014. 5
- [27] J. D. Hunter. Matplotlib: A 2d graphics environment. *Computing in Science & Engineering*, 9(3):90–95, 2007. 14
- [28] A Krizhevsky and G Hinton. Learning multiple layers of features from tiny images. 2009. 3
- [29] Brenden M Lake, Ruslan Salakhutdinov, and Joshua B Tenenbaum. Human-level concept learning through probabilistic program induction. *Science*, 350(6266):1332–1338, Dec. 2015. 3
- [30] Brenden M Lake, Ruslan Salakhutdinov, and Joshua B Tenenbaum. The omniglot challenge: a 3-year progress report. Feb. 2019. 3
- [31] Kwonjoon Lee, Subhansu Maji, Avinash Ravichandran, and Stefano Soatto. Meta-learning with differentiable convex op-

- timization. In *Proceedings of the IEEE Conference on Computer Vision and Pattern Recognition*, pages 10657–10665, 2019. 3, 5
- [32] Yoonho Lee and Seungjin Choi. Gradient-based meta-learning with learned layerwise metric and subspace. volume 80 of *Proceedings of Machine Learning Research*, pages 2927–2936, Stockholmsmässan, Stockholm Sweden, 10–15 Jul 2018. PMLR. 2
- [33] Zhenguo Li, Fengwei Zhou, Fei Chen, and Hang Li. Meta-SGD: Learning to learn quickly for Few-Shot learning. July 2017. 2
- [34] Moshe Lichtenstein, Prasanna Sattigeri, Rogerio Feris, Raja Giryes, and Leonid Karlinsky. TAFSSL: Task-Adaptive feature Sub-Space learning for few-shot classification. Mar. 2020. 3
- [35] David J C MacKay. *Information Theory, Inference & Learning Algorithms*. Cambridge University Press, USA, 2002. 4
- [36] Subhansu Maji, Esa Rahtu, Juho Kannala, Matthew Blaschko, and Andrea Vedaldi. Fine-Grained visual classification of aircraft. June 2013. 3
- [37] E G Miller, N E Matsakis, and P A Viola. Learning from one example through shared densities on transforms. In *Proceedings IEEE Conference on Computer Vision and Pattern Recognition. CVPR 2000 (Cat. No.PR00662)*, volume 1, pages 464–471 vol.1, June 2000. 1, 2
- [38] George A Miller, Richard Beckwith, Christiane Fellbaum, Derek Gross, and Katherine J Miller. Introduction to WordNet: An on-line lexical database \*. *Int J Lexicography*, 3(4):235–244, 1990. 3
- [39] Nikhil Mishra, Mostafa Rohaninejad, Xi Chen, and Pieter Abbeel. A simple neural attentive meta-learner. In *International Conference on Learning Representations*, 2018. 5
- [40] Jesse Mu, Percy Liang, and Noah Goodman. Shaping visual representations with language for few-shot classification. In *Proceedings of the 58th Annual Meeting of the Association for Computational Linguistics*, pages 4823–4830, Online, July 2020. Association for Computational Linguistics. 2
- [41] M Nilsback and A Zisserman. A visual vocabulary for flower classification. In *2006 IEEE Computer Society Conference on Computer Vision and Pattern Recognition (CVPR’06)*, volume 2, pages 1447–1454, June 2006. 3
- [42] Boris Oreshkin, Pau Rodríguez López, and Alexandre Lacoste. TADAM: Task dependent adaptive metric for improved few-shot learning. In S Bengio, H Wallach, H Larochelle, K Grauman, N Cesa-Bianchi, and R Garnett, editors, *Advances in Neural Information Processing Systems 31*, pages 721–731. Curran Associates, Inc., 2018. 1, 3
- [43] Pedro A Ortega, Jane X Wang, Mark Rowland, Tim Genewein, Zeb Kurth-Nelson, Razvan Pascanu, Nicolas Heess, Joel Veness, Alex Pritzel, Pablo Sprechmann, Siddhant M Jayakumar, Tom McGrath, Kevin Miller, Mohammad Azar, Ian Osband, Neil Rabinowitz, András György, Silvia Chiappa, Simon Osindero, Yee Whye Teh, Hado van Hasselt, Nando de Freitas, Matthew Botvinick, and Shane Legg. Meta-learning of sequential strategies. May 2019. 2
- [44] Eunbyung Park and Junier B Oliva. Meta-curvature. In *Advances in Neural Information Processing Systems*, pages 3314–3324, 2019. 2
- [45] Adam Paszke, Sam Gross, Francisco Massa, Adam Lerer, James Bradbury, Gregory Chanan, Trevor Killeen, Zeming Lin, Natalia Gimelshein, Luca Antiga, Alban Desmaison, Andreas Kopf, Edward Yang, Zachary DeVito, Martin Raison, Alykhan Tejani, Sasank Chilamkurthy, Benoit Steiner, Lu Fang, Junjie Bai, and Soumith Chintala. Pytorch: An imperative style, high-performance deep learning library. In *Advances in Neural Information Processing Systems 32*, pages 8024–8035. Curran Associates, Inc., 2019. 14
- [46] F. Pedregosa, G. Varoquaux, A. Gramfort, V. Michel, B. Thirion, O. Grisel, M. Blondel, P. Prettenhofer, R. Weiss, V. Dubourg, J. Vanderplas, A. Passos, D. Cournapeau, M. Brucher, M. Perrot, and E. Duchesnay. Scikit-learn: Machine learning in Python. *Journal of Machine Learning Research*, 12:2825–2830, 2011. 14
- [47] Viraj Prabhu, Anitha Kannan, Murali Ravuri, Manish Chaplain, David Sontag, and Xavier Amatriain. Few-Shot learning for dermatological disease diagnosis. 106:532–552, 2019. 2
- [48] Hang Qi, Matthew Brown, and David G Lowe. Low-shot learning with imprinted weights. In *Proceedings of the IEEE conference on computer vision and pattern recognition*, pages 5822–5830, 2018. 2
- [49] Aniruddh Raghu, Maithra Raghu, Samy Bengio, and Oriol Vinyals. Rapid learning or feature reuse? towards understanding the effectiveness of maml. In *International Conference on Learning Representations*, 2020. 1, 2, 8
- [50] Aravind Rajeswaran, Chelsea Finn, Sham M Kakade, and Sergey Levine. Meta-learning with implicit gradients. In *Advances in Neural Information Processing Systems*, pages 113–124, 2019. 2
- [51] Kate Rakelly, Aurick Zhou, Chelsea Finn, Sergey Levine, and Deirdre Quillen. Efficient off-policy meta-reinforcement learning via probabilistic context variables. volume 97 of *Proceedings of Machine Learning Research*, pages 5331–5340, Long Beach, California, USA, 09–15 Jun 2019. PMLR. 2
- [52] Sachin Ravi and Hugo Larochelle. Optimization as a model for few-shot learning. In *International Conference on Learning Representations, 2017*, 2017. 2, 3
- [53] Mengye Ren, Sachin Ravi, Eleni Triantafillou, Jake Snell, Kevin Swersky, Josh B. Tenenbaum, Hugo Larochelle, and Richard S. Zemel. Meta-learning for semi-supervised few-shot classification. In *International Conference on Learning Representations*, 2018. 1, 3
- [54] Pau Rodríguez, Issam Laradji, Alexandre Drouin, and Alexandre Lacoste. Embedding propagation: Smoother manifold for few-shot classification. *European Conference on Computer Vision*, 2020. 3
- [55] Olga Russakovsky, Jia Deng, Hao Su, Jonathan Krause, Sanjeev Satheesh, Sean Ma, Zhiheng Huang, Andrej Karpathy, Aditya Khosla, Michael Bernstein, Alexander C Berg, and Li Fei-Fei. ImageNet large scale visual recognition challenge. *Int. J. Comput. Vis.*, 115(3):211–252, Dec. 2015. 3
- [56] Andrei A. Rusu, Dushyant Rao, Jakub Sygnowski, Oriol Vinyals, Razvan Pascanu, Simon Osindero, and Raia Hadsell. Meta-learning with latent embedding optimization. In

- International Conference on Learning Representations*, 2019. 2
- [57] Sara Sabour, Nicholas Frosst, and Geoffrey E Hinton. Dynamic routing between capsules. *NIPS*, 2017. 3
- [58] Mandana Samiei, Tobias Würfl, Tristan Deleu, Martin Weiss, Francis Dutil, Thomas Fevens, Geneviève Boucher, Sebastien Lemieux, and Joseph Paul Cohen. The TCGA Meta-Dataset clinical benchmark. Oct. 2019. 3
- [59] Adam Santoro, Sergey Bartunov, Matthew Botvinick, Daan Wierstra, and Timothy Lillicrap. Meta-Learning with Memory-Augmented neural networks. In Maria Florina Balcan and Kilian Q Weinberger, editors, *Proceedings of The 33rd International Conference on Machine Learning*, volume 48 of *Proceedings of Machine Learning Research*, pages 1842–1850, New York, New York, USA, 2016. PMLR. 2
- [60] Juergen Schmidhuber. *Evolutionary Principles in Self-Referential Learning*. PhD thesis, 1987. 2
- [61] Brigit Schroeder and Yin Cui. *FGVCx fungi classification challenge 2018*, 2018. 3
- [62] Ozan Sener and Vladlen Koltun. Multi-Task learning as Multi-Objective optimization. In S Bengio, H Wallach, H Larochelle, K Grauman, N Cesa-Bianchi, and R Garnett, editors, *Advances in Neural Information Processing Systems*, volume 31, pages 527–538. Curran Associates, Inc., 2018. 3
- [63] Jake Snell, Kevin Swersky, and Richard Zemel. Prototypical networks for few-shot learning. In *Advances in neural information processing systems*, pages 4077–4087, 2017. 3, 5
- [64] Milan Sulc, Lukas Picek, Jiri Matas, Thomas Jeppesen, and Jacob Heilmann-Clausen. Fungi recognition: A practical use case. In *The IEEE Winter Conference on Applications of Computer Vision*, pages 2316–2324, 2020. 3
- [65] Christian Szegedy, Wei Liu, Yangqing Jia, Pierre Sermanet, Scott Reed, Dragomir Anguelov, Dumitru Erhan, Vincent Vanhoucke, and Andrew Rabinovich. Going deeper with convolutions. In *Proceedings of the IEEE conference on computer vision and pattern recognition*, pages 1–9, 2015. 5
- [66] Yonglong Tian, Yue Wang, Dilip Krishnan, Joshua B. Tenenbaum, and Phillip Isola. Rethinking few-shot image classification: A good embedding is all you need? In Andrea Vedaldi, Horst Bischof, Thomas Brox, and Jan-Michael Frahm, editors, *Computer Vision – ECCV 2020*, pages 266–282, Cham, 2020. Springer International Publishing. 1, 3, 8
- [67] The torchvision contributors. torchvision. <https://github.com/pytorch/vision>, 2020. [Online; accessed 20-November-2020]. 14
- [68] Eleni Triantafillou, Tyler Zhu, Vincent Dumoulin, Pascal Lamblin, Utku Evci, Kelvin Xu, Ross Goroshin, Carles Gelada, Kevin Swersky, Pierre-Antoine Manzagol, and Hugo Larochelle. Meta-dataset: A dataset of datasets for learning to learn from few examples. In *International Conference on Learning Representations*, 2020. 1, 3
- [69] Guido Van Rossum and Fred L. Drake. *Python 3 Reference Manual*. CreateSpace, Scotts Valley, CA, 2009. 14
- [70] Joaquin Vanschoren. Meta-Learning: A survey. Oct. 2018. 2
- [71] Oriol Vinyals, Charles Blundell, Timothy Lillicrap, Koray Kavukcuoglu, and Daan Wierstra. Matching networks for one shot learning. In D D Lee, M Sugiyama, U V Luxburg, I Guyon, and R Garnett, editors, *Advances in Neural Information Processing Systems 29*, pages 3630–3638. Curran Associates, Inc., 2016. 1, 3
- [72] Yan Wang, Wei-Lun Chao, Kilian Q Weinberger, and Laurens van der Maaten. SimpleShot: Revisiting Nearest-Neighbor classification for Few-Shot learning. Nov. 2019. 3
- [73] Yaqing Wang, Quanming Yao, James T Kwok, and Lionel M Ni. Generalizing from a few examples: A survey on few-shot learning. *ACM Comput. Surv.*, 53(3):1–34, June 2020. 2
- [74] Jason Wei and Kai Zou. EDA: Easy data augmentation techniques for boosting performance on text classification tasks. In *Proceedings of the 2019 Conference on Empirical Methods in Natural Language Processing and the 9th International Joint Conference on Natural Language Processing (EMNLP-IJCNLP)*, pages 6381–6387, Stroudsburg, PA, USA, 2019. Association for Computational Linguistics. 2
- [75] Peter Welinder, Steve Branson, Takeshi Mita, Catherine Wah, Florian Schroff, Serge Belongie, and Pietro Perona. Caltech-UCSD birds 200. 2010. 3
- [76] Sen Wu, Hongyang R Zhang, and Christopher Ré. Understanding and improving information transfer in Multi-Task learning. Sept. 2019. 7
- [77] Chen Xing, Negar Rostamzadeh, Boris Oreshkin, and Pedro O O Pinheiro. Adaptive cross-modal few-shot learning. *Advances in Neural Information Processing Systems*, 32:4847–4857, 2019. 2
- [78] Jincheng Xu and Qingfeng Du. Learning transferable features in meta-learning for few-shot text classification. *Pattern Recognit. Lett.*, 135:271–278, July 2020. 2
- [79] Han-Jia Ye, Hexiang Hu, De-Chuan Zhan, and Fei Sha. Few-shot learning via embedding adaptation with set-to-set functions. In *Proceedings of the IEEE/CVF Conference on Computer Vision and Pattern Recognition*, pages 8808–8817, 2020. 3
- [80] Jaesik Yoon, Taesup Kim, Ousmane Dia, Sungwoong Kim, Yoshua Bengio, and Sungjin Ahn. Bayesian Model-Agnostic Meta-Learning. In S Bengio, H Wallach, H Larochelle, K Grauman, N Cesa-Bianchi, and R Garnett, editors, *Advances in Neural Information Processing Systems*, volume 31, pages 7332–7342. Curran Associates, Inc., 2018. 2
- [81] Mo Yu, Xiaoxiao Guo, Jinfeng Yi, Shiyu Chang, Saloni Potdar, Yu Cheng, Gerald Tesauro, Haoyu Wang, and Bowen Zhou. Diverse Few-Shot text classification with multiple metrics. In *Proceedings of the 2018 Conference of the North American Chapter of the Association for Computational Linguistics: Human Language Technologies, Volume 1 (Long Papers)*, pages 1206–1215, New Orleans, Louisiana, June 2018. Association for Computational Linguistics. 2
- [82] Xiaohua Zhai, Joan Puigcerver, Alexander Kolesnikov, Pierre Ruyssen, Carlos Riquelme, Mario Lucic, Josip Djolonga, Andre Susano Pinto, Maxim Neumann, Alexey Dosovitskiy, Lucas Beyer, Olivier Bachem, Michael Tschannen, Marcin Michalski, Olivier Bousquet, Sylvain Gelly, and Neil Houlsby. A large-scale study of representation learning with the visual task adaptation benchmark. Oct. 2019. 3
- [83] Chi Zhang, Yujun Cai, Guosheng Lin, and Chunhua Shen. Deepemd: Few-shot image classification with differentiable



earth mover's distance and structured classifiers. In *Proceedings of the IEEE/CVF Conference on Computer Vision and Pattern Recognition*, pages 12203–12213, 2020. [3](#)

- [84] Allan Zhou, Tom Knowles, and Chelsea Finn. Meta-Learning symmetries by reparameterization. July 2020. [2](#)
- [85] Luisa Zintgraf, Kyriacos Shiarli, Vitaly Kurin, Katja Hofmann, and Shimon Whiteson. Fast context adaptation via meta-learning. volume 97 of *Proceedings of Machine Learning Research*, pages 7693–7702, Long Beach, California, USA, 09–15 Jun 2019. PMLR. [2](#)

## A. Supplementary Material

The following sections provide additional details on our experiments, our implementations, and the tasksets generated with our method.

### A.1. Experimental Details

### A.2. Controlling Information Overlap

For results reported in Figure 2 we train the Multiclass network for 200 epochs on the train classes, and measure test accuracy over 600 test tasks with the weights obtained at the best validation epoch. For optimization, we use Adam with a tuned learning rate and other hyper-parameters set to the default values in PyTorch. We do not use weight decay regularization nor decay the learning rate, and set the mini-batch size to 64.

For the PCA projections of Figure 3, we use the PCA implementation in scikit-learn with default hyper-parameters and simply set `ncomponents=2`. When reporting  $\|\mu_{\text{train}} - \mu_{\text{test}}\|$ , we measure the Euclidean distance in the original embedding space not the projected one.

Since we do not need to optimize their parameters, we use Gaussians to measure correlation between divergence and accuracies in Table 2. We estimate the means and covariance from the class embeddings, and use a small diagonal damping factor of 0.001 to ensure numerical stability.

### A.3. Comparing Semantic vs Embedding Clusters

For Table 4, the label *Easy* corresponds to  $D = 0.04$ , *Hard* to  $D = 0.96$ . For *Random*, we randomly partition classes among train, validation, and test sets which is equivalent to  $D = 0$ . The CNN4 and ResNet12 implementations are provided with our code release.

When comparing clustering trees in Table 3, we use the agglomerative clustering implementation found in scikit-learn, and set the linkage argument to `'ward'`. We parse the structures in the following 2 files to build the WordNet graph over ImageNet-1k:

- <http://www.image-net.org/api/xml/ReleaseStatus.xml> and
- [http://www.image-net.org/api/xml/structure\\_released.xml](http://www.image-net.org/api/xml/structure_released.xml),

and prune the graph to discard leaves irrelevant to ImageNet-1k synsets.

### A.4. Is a Good Embedding Really Enough?

For each method, the slopes in Table 5 are computed using the test accuracies when varying  $R$  from 0.04 to 0.96. In Table 1, we report the test accuracies when  $D = 0.96$ .

## A.5. Code Release

With this submission, we include implementation for ATG, as well as parallelized implementations for popular few-shot learning algorithms. (MAML, ANIL, and ProtoNet)

The few-shot learning implementations proceed one task at a time. Before processing the task, the model is replicated across all GPUs; then, the data of the task is split across GPUs and processed by each of the replicas independently. (This parallelization is made simple thanks to PyTorch’s `DataParallel` wrapper.) Finally, the output of each replica is gathered on the first GPU to compute the cross-entropy loss. Those implementations are available in `maml.py`, `anil.py`, and `protonet.py`.

The ATG implementation is provided in `atg.py`. It (and our other implementations) can be ran as-is, using the python command:

```
python cvpr_code/atg.py
```

For more details on our implementations, please refer to the included `README.md` file. As mentioned in the main text, our implementations are available at <http://seba1511.net/projects/atg>.

### A.5.1 Software Acknowledgement

This manuscript is made possible thanks to the following open-source software: Python [69], Numpy [23], PyTorch [45], torchvision [67], scikit-learn [46], learn2learn [4], and matplotlib [27].

## A.6. Taskset Partitions

We describe the tasksets generated by our method for different degrees of difficulty, obtained for different values of  $R = 0.04, 0.32, 0.64, 0.96$ . The following tables provide the train, validation, and test class partitions for

- Table 6 for CIFAR100 as implemented in torchvision,
- Table 7 for mini-ImageNet as implemented in learn2learn,
- Table 8 for EMNIST as implemented in torchvision,
- Table 9 for LFW10 as implemented in scikit-learn, and
- Tables 10 and 11 for tiered-ImageNet as implemented in learn2learn.

All those partitions are obtained with ATG, with the following implementation details. First, we normalize the class embeddings to unit norm; then, optimize  $\mu_{\text{train}}$  and  $\mu_{\text{test}}$  to minimize the objective  $J$ . To that end, we use SGD with a 0.1 learning rate and momentum set to 0.9 for 7,000 iterations.

Table 6: Taskset partitions for CIFAR100.

Setting	Taskset	Classes
D = 0.04	Train	37, 39, 41, 89, 74, 15, 19, 8, 31, 95, 77, 38, 32, 17, 12, 90, 42, 84, 75, 25, 20, 0, 71, 69, 4, 86, 63, 80, 55, 40, 5, 50, 94, 87, 72, 34, 76, 13, 10, 81, 88, 58, 65, 22, 3, 66, 64, 61, 16, 28, 9, 2, 43, 21, 46, 97, 11, 35, 36, 98
	Validation	47, 91, 56, 83, 59, 26, 1, 93, 27, 73, 14, 48, 30, 70, 68, 54, 67, 6, 85, 57
	Test	52, 82, 44, 96, 60, 33, 49, 45, 18, 7, 92, 29, 51, 78, 62, 79, 24, 23, 53, 99
D = 0.32	Train	99, 42, 53, 32, 23, 4, 75, 63, 48, 68, 80, 34, 50, 55, 85, 8, 95, 41, 72, 89, 0, 39, 37, 88, 84, 3, 17, 20, 66, 65, 43, 40, 90, 12, 25, 64, 69, 21, 71, 10, 28, 86, 97, 5, 61, 76, 94, 2, 35, 46, 11, 16, 22, 9, 87, 98, 13, 81, 36, 58
	Validation	47, 44, 26, 7, 27, 18, 56, 14, 29, 1, 78, 62, 24, 60, 15, 49, 38, 67, 73, 57
	Test	52, 96, 33, 82, 59, 93, 91, 83, 45, 51, 79, 70, 92, 6, 54, 74, 19, 30, 77, 31
D = 0.64	Train	43, 32, 50, 55, 75, 3, 57, 30, 72, 60, 88, 53, 99, 21, 49, 66, 73, 23, 65, 8, 97, 64, 0, 35, 95, 41, 2, 85, 48, 68, 84, 89, 11, 98, 28, 46, 40, 39, 36, 20, 10, 37, 17, 61, 25, 69, 90, 71, 9, 16, 12, 86, 22, 5, 94, 76, 87, 81, 13, 58
	Validation	96, 26, 33, 27, 93, 6, 78, 70, 14, 45, 62, 38, 83, 56, 92, 31, 77, 42, 67, 80
	Test	52, 47, 44, 7, 59, 51, 18, 29, 79, 24, 82, 15, 19, 74, 91, 1, 54, 4, 34, 63
D = 0.96	Train	55, 35, 92, 83, 72, 75, 82, 65, 1, 32, 56, 91, 2, 98, 64, 11, 67, 36, 46, 57, 30, 8, 53, 60, 23, 99, 49, 73, 41, 28, 89, 84, 0, 48, 85, 40, 95, 10, 39, 68, 20, 61, 25, 17, 37, 9, 16, 90, 86, 22, 69, 5, 94, 71, 12, 76, 58, 13, 81, 87
	Validation	96, 19, 15, 31, 6, 7, 44, 51, 21, 27, 62, 24, 4, 93, 74, 54, 14, 42, 50, 63
	Test	52, 43, 38, 26, 47, 33, 34, 3, 70, 59, 78, 29, 79, 45, 80, 97, 88, 66, 18, 77

Table 7: Taskset partitions for mini-ImageNet.

Setting	Taskset	Classes
D = 0.04	Train	70, 87, 26, 31, 69, 78, 4, 73, 28, 83, 43, 46, 36, 14, 58, 49, 50, 8, 65, 9, 64, 2, 67, 39, 76, 88, 18, 91, 47, 42, 29, 68, 25, 12, 94, 99, 98, 11, 92, 61, 74, 71, 52, 77, 85, 37, 56, 66, 93, 5, 17, 97, 48, 24, 21, 20, 30, 95, 60, 84
	Validation	35, 96, 53, 15, 63, 1, 23, 22, 54, 13, 82, 79, 40, 44, 51, 32, 6, 89, 55, 80
	Test	7, 33, 19, 86, 72, 27, 90, 59, 57, 45, 0, 41, 81, 34, 75, 38, 3, 10, 62, 16
D = 0.32	Train	40, 22, 76, 66, 75, 85, 2, 23, 58, 36, 44, 91, 48, 39, 94, 72, 97, 34, 74, 17, 53, 90, 25, 92, 24, 70, 51, 98, 84, 64, 60, 43, 37, 29, 89, 69, 52, 41, 47, 57, 73, 26, 96, 28, 93, 55, 46, 31, 32, 42, 38, 61, 49, 50, 77, 95, 71, 56, 30, 21
	Validation	19, 15, 63, 10, 20, 86, 82, 5, 88, 1, 27, 33, 35, 45, 12, 11, 68, 79, 80, 4
	Test	3, 13, 62, 16, 59, 18, 7, 54, 14, 81, 8, 6, 9, 83, 99, 0, 87, 65, 67, 78
D = 0.64	Train	4, 66, 2, 80, 76, 60, 40, 48, 23, 91, 22, 97, 36, 94, 75, 44, 84, 25, 17, 39, 74, 24, 29, 92, 90, 98, 34, 64, 72, 37, 53, 51, 70, 43, 47, 52, 89, 69, 73, 26, 93, 41, 55, 42, 57, 28, 61, 38, 46, 96, 32, 49, 50, 31, 77, 95, 56, 71, 30, 21
	Validation	19, 13, 63, 59, 16, 10, 54, 81, 14, 8, 7, 27, 11, 33, 67, 65, 35, 85, 78, 58
	Test	3, 62, 20, 15, 18, 86, 5, 82, 88, 1, 99, 12, 9, 83, 87, 68, 0, 6, 45, 79
D = 0.96	Train	4, 45, 25, 6, 76, 48, 66, 91, 23, 84, 29, 80, 97, 44, 40, 22, 24, 94, 92, 36, 74, 39, 90, 75, 17, 64, 51, 47, 37, 98, 89, 52, 53, 72, 42, 34, 43, 69, 70, 73, 55, 26, 38, 93, 57, 50, 61, 41, 49, 46, 95, 28, 96, 32, 77, 31, 30, 56, 71, 21
	Validation	62, 20, 59, 86, 81, 18, 16, 82, 88, 8, 12, 27, 67, 87, 33, 83, 65, 0, 78, 58
	Test	3, 19, 63, 13, 15, 5, 10, 54, 1, 14, 99, 85, 9, 68, 79, 7, 60, 11, 2, 35

Table 8: Taskset partitions for EMNIST.

Setting	Taskset	Classes
D = 0.04	Train	61, 52, 17, 45, 8, 32, 13, 36, 44, 1, 19, 56, 60, 0, 18, 24, 9, 16, 11, 50, 22, 12, 57, 53, 38, 6, 33, 48, 27, 58, 41, 59, 49, 10, 54, 40, 28, 3
	Validation	55, 20, 7, 46, 42, 23, 34, 30, 31, 26, 14, 15
	Test	29, 21, 5, 35, 39, 25, 51, 37, 4, 2, 43, 47
D = 0.32	Train	31, 9, 17, 27, 34, 40, 14, 11, 4, 55, 57, 46, 5, 2, 60, 10, 61, 21, 53, 16, 8, 15, 39, 43, 19, 37, 33, 59, 41, 45, 6, 47, 54, 44, 18, 1, 3, 28
	Validation	48, 0, 24, 7, 25, 32, 56, 36, 42, 20, 38, 35
	Test	22, 29, 50, 51, 30, 23, 26, 13, 58, 49, 12, 52
D = 0.64	Train	23, 28, 35, 17, 19, 41, 30, 47, 61, 40, 1, 44, 56, 18, 49, 27, 32, 11, 8, 45, 43, 42, 9, 58, 37, 13, 3, 16, 52, 24, 2, 50, 0, 6, 10, 39, 36, 26
	Validation	5, 20, 60, 53, 46, 55, 21, 33, 4, 48, 12, 51
	Test	29, 34, 31, 14, 7, 57, 15, 22, 25, 59, 54, 38
D = 0.96	Train	19, 37, 1, 61, 18, 44, 45, 8, 25, 16, 6, 30, 11, 17, 40, 43, 3, 22, 51, 48, 42, 56, 23, 9, 27, 52, 2, 13, 39, 49, 32, 24, 58, 50, 0, 10, 26, 36
	Validation	29, 34, 54, 20, 15, 55, 53, 7, 33, 41, 38, 47
	Test	5, 21, 14, 28, 60, 31, 46, 57, 4, 12, 59, 35

Table 9: Taskset partitions for LFW10.

Setting	Taskset	Classes
D = 0.04	Train	128, 133, 13, 100, 7, 67, 91, 140, 122, 66, 22, 6, 5, 42, 88, 0, 156, 107, 81, 149, 41, 148, 2, 80, 153, 62, 98, 83, 71, 123, 109, 58, 53, 84, 25, 35, 136, 8, 141, 146, 57, 56, 135, 157, 129, 143, 34, 117, 93, 4, 52, 118, 137, 73, 126, 15, 101, 97, 26, 138, 60, 50, 147, 127, 95, 104, 78, 134, 119, 121, 132, 33, 139, 31, 54, 124, 96, 30, 87, 44, 11, 27, 103, 39, 14, 38, 142, 89, 74, 70, 125, 69, 152, 23, 116, 120
	Validation	63, 36, 111, 47, 9, 61, 28, 40, 68, 45, 21, 51, 108, 10, 105, 77, 75, 115, 144, 106, 12, 59, 37, 86, 130, 113, 49, 114, 46, 112, 16
	Test	82, 65, 76, 92, 90, 48, 110, 20, 17, 72, 79, 24, 3, 94, 18, 150, 29, 19, 145, 99, 64, 55, 155, 131, 154, 1, 43, 32, 85, 151, 102
D = 0.32	Train	77, 109, 122, 42, 40, 94, 85, 64, 2, 128, 81, 80, 118, 55, 17, 97, 54, 107, 153, 123, 83, 30, 20, 71, 25, 135, 56, 9, 156, 58, 101, 137, 96, 34, 115, 0, 117, 31, 22, 78, 138, 57, 62, 126, 38, 52, 27, 146, 129, 11, 144, 35, 41, 91, 143, 124, 114, 33, 132, 60, 95, 50, 87, 6, 147, 127, 134, 44, 8, 84, 53, 73, 93, 103, 139, 98, 157, 121, 89, 26, 119, 14, 4, 141, 69, 15, 23, 104, 116, 142, 152, 125, 39, 120, 74, 70
	Validation	48, 110, 92, 99, 82, 37, 111, 45, 59, 67, 1, 88, 19, 12, 13, 108, 140, 3, 24, 131, 133, 66, 79, 72, 90, 29, 130, 16, 7, 76, 150
	Test	155, 68, 36, 105, 102, 28, 63, 18, 51, 113, 47, 75, 145, 43, 5, 65, 61, 106, 100, 10, 86, 154, 148, 46, 112, 136, 21, 149, 32, 151, 49
D = 0.64	Train	81, 16, 49, 150, 66, 21, 137, 25, 52, 102, 71, 54, 22, 58, 1, 136, 97, 118, 107, 99, 83, 40, 111, 57, 17, 96, 33, 134, 56, 62, 117, 87, 123, 133, 115, 138, 156, 78, 38, 64, 34, 80, 60, 2, 42, 144, 20, 124, 76, 31, 35, 50, 147, 9, 6, 0, 89, 126, 44, 143, 103, 116, 26, 91, 127, 84, 95, 85, 93, 146, 23, 114, 139, 53, 73, 8, 98, 141, 14, 119, 41, 15, 121, 132, 142, 69, 125, 152, 4, 104, 39, 129, 157, 120, 74, 70
	Validation	36, 59, 68, 75, 29, 61, 149, 51, 140, 67, 113, 110, 154, 153, 148, 122, 77, 79, 19, 135, 145, 24, 94, 65, 130, 32, 151, 27, 82, 46, 108
	Test	28, 155, 92, 13, 106, 131, 3, 18, 5, 7, 47, 100, 12, 63, 45, 112, 72, 30, 105, 43, 48, 55, 88, 128, 37, 101, 10, 109, 90, 86, 11
D = 0.96	Train	56, 83, 62, 43, 55, 110, 30, 87, 107, 57, 134, 16, 133, 64, 101, 42, 82, 66, 99, 137, 34, 20, 50, 111, 25, 96, 156, 2, 79, 76, 117, 11, 91, 33, 0, 32, 27, 10, 6, 53, 138, 102, 144, 26, 71, 31, 9, 116, 54, 98, 60, 97, 40, 114, 39, 15, 136, 143, 8, 89, 141, 123, 35, 80, 103, 84, 142, 38, 147, 78, 119, 95, 124, 93, 157, 74, 104, 41, 139, 146, 126, 73, 121, 127, 152, 4, 85, 23, 44, 132, 125, 129, 120, 14, 69, 70
	Validation	36, 92, 28, 106, 72, 140, 12, 24, 18, 100, 3, 75, 61, 63, 5, 47, 48, 17, 45, 88, 49, 90, 1, 22, 37, 19, 148, 58, 115, 130, 109
	Test	7, 155, 59, 67, 94, 113, 149, 13, 131, 105, 135, 65, 122, 29, 68, 51, 21, 108, 150, 153, 151, 145, 128, 154, 52, 112, 86, 77, 81, 46, 118



Table 10: Taskset partitions for tiered-ImageNet.

Setting	Taskset	Classes
D = 0.04	Train	163, 403, 375, 148, 381, 431, 160, 363, 187, 499, 412, 321, 103, 264, 553, 318, 560, 410, 448, 97, 173, 179, 368, 331, 442, 557, 165, 457, 376, 337, 116, 325, 91, 598, 227, 559, 150, 77, 36, 118, 104, 411, 212, 8, 9, 188, 418, 278, 509, 498, 383, 82, 508, 473, 468, 266, 133, 310, 138, 436, 385, 423, 584, 490, 263, 520, 358, 238, 195, 297, 510, 193, 497, 141, 354, 283, 391, 426, 320, 299, 393, 32, 356, 603, 433, 5, 400, 192, 29, 251, 486, 512, 382, 384, 157, 558, 137, 555, 366, 482, 117, 265, 170, 67, 446, 105, 447, 319, 352, 462, 351, 42, 336, 268, 541, 52, 394, 539, 593, 342, 456, 216, 151, 214, 416, 276, 296, 361, 395, 98, 581, 196, 369, 249, 554, 390, 537, 570, 396, 267, 569, 261, 576, 204, 181, 286, 115, 220, 126, 480, 347, 16, 30, 346, 322, 524, 145, 538, 277, 372, 22, 566, 516, 84, 246, 229, 496, 59, 589, 472, 112, 125, 406, 159, 288, 518, 421, 466, 7, 475, 38, 211, 111, 69, 350, 364, 444, 262, 443, 129, 333, 20, 328, 329, 134, 463, 123, 89, 85, 275, 341, 491, 100, 314, 389, 450, 437, 607, 335, 224, 345, 451, 413, 428, 551, 128, 174, 359, 483, 71, 289, 580, 386, 234, 404, 340, 75, 536, 543, 591, 365, 408, 217, 106, 18, 215, 155, 15, 92, 198, 432, 392, 454, 306, 79, 168, 176, 237, 21, 343, 371, 47, 152, 547, 525, 94, 316, 33, 63, 334, 99, 527, 360, 53, 402, 323, 419, 272, 37, 597, 164, 529, 605, 434, 449, 532, 517, 295, 500, 202, 80, 110, 130, 144, 357, 573, 201, 146, 344, 96, 315, 332, 552, 549, 60, 250, 535, 232, 222, 167, 226, 519, 544, 355, 308, 252, 131, 269, 158, 46, 515, 414, 76, 61, 312, 28, 132, 240, 182, 301, 501, 489, 505, 338, 567, 210, 439, 142, 467, 190, 50, 578, 180, 565, 487, 455, 546, 19, 253, 40, 285, 41, 317, 175, 293, 225, 161, 495, 239, 219, 424, 25, 184, 279, 247, 542, 572, 207, 31, 587, 66, 54, 185, 550, 453, 563
	Validation	588, 55, 504, 493, 209, 136, 460, 399, 2, 113, 339, 292, 503, 484, 459, 122, 90, 304, 156, 313, 245, 415, 135, 166, 602, 464, 4, 213, 307, 291, 430, 401, 441, 548, 526, 58, 273, 465, 282, 13, 330, 425, 154, 49, 458, 178, 68, 601, 119, 388, 203, 86, 230, 513, 294, 81, 280, 305, 481, 88, 309, 420, 51, 574, 139, 189, 507, 17, 143, 87, 586, 438, 200, 14, 248, 387, 577, 440, 257, 600, 521, 422, 169, 534, 78, 575, 397, 107, 44, 10, 101, 471, 523, 327, 405, 108, 72, 56, 595, 579, 311, 378, 26, 6, 284, 485, 43, 377, 303, 221, 242, 102, 429, 208, 147, 290, 177, 479, 109, 27, 120
	Test	445, 583, 348, 259, 199, 93, 162, 514, 604, 571, 461, 469, 300, 585, 545, 74, 530, 23, 62, 228, 582, 511, 494, 83, 270, 271, 353, 470, 256, 594, 435, 281, 606, 274, 3, 191, 153, 124, 528, 452, 502, 260, 476, 374, 409, 171, 599, 540, 236, 298, 57, 326, 596, 258, 140, 255, 35, 287, 1, 205, 362, 522, 194, 45, 114, 370, 561, 218, 183, 233, 206, 65, 568, 186, 417, 592, 492, 24, 243, 127, 427, 95, 64, 380, 302, 254, 478, 590, 73, 367, 379, 121, 556, 149, 488, 11, 477, 172, 223, 197, 39, 407, 373, 231, 474, 48, 235, 244, 506, 349, 562, 0, 324, 241, 564, 34, 533, 70, 12, 531, 398
D = 0.32	Train	256, 34, 135, 249, 17, 322, 229, 403, 511, 234, 422, 464, 468, 215, 287, 198, 16, 18, 122, 452, 482, 84, 423, 12, 265, 481, 439, 59, 27, 426, 362, 33, 416, 208, 20, 512, 280, 361, 513, 237, 446, 288, 314, 411, 559, 421, 574, 92, 309, 52, 86, 383, 522, 168, 340, 320, 507, 306, 323, 365, 497, 103, 569, 186, 582, 181, 604, 410, 506, 562, 330, 71, 364, 354, 193, 579, 264, 75, 457, 195, 85, 390, 42, 328, 341, 176, 461, 286, 396, 311, 310, 98, 112, 272, 67, 523, 8, 530, 470, 69, 370, 592, 120, 108, 499, 393, 350, 127, 601, 76, 137, 428, 73, 160, 212, 442, 232, 22, 57, 472, 585, 316, 543, 595, 220, 602, 520, 124, 68, 105, 369, 503, 502, 87, 534, 177, 325, 389, 599, 381, 179, 531, 458, 427, 116, 515, 21, 134, 456, 4, 5, 91, 333, 117, 319, 404, 261, 145, 576, 568, 53, 560, 133, 366, 571, 477, 216, 372, 387, 269, 167, 490, 524, 516, 344, 268, 15, 30, 106, 510, 538, 408, 437, 359, 494, 541, 539, 412, 544, 152, 444, 118, 475, 164, 414, 80, 447, 518, 329, 243, 241, 151, 210, 600, 533, 238, 360, 297, 591, 432, 31, 41, 558, 448, 252, 386, 315, 148, 462, 121, 352, 555, 556, 607, 590, 371, 476, 551, 201, 305, 170, 554, 240, 225, 224, 37, 537, 596, 174, 606, 454, 278, 449, 47, 501, 480, 50, 345, 150, 392, 97, 338, 196, 79, 581, 163, 89, 406, 184, 146, 566, 451, 593, 96, 312, 580, 219, 129, 474, 155, 498, 394, 38, 295, 419, 110, 28, 536, 573, 400, 443, 402, 491, 605, 308, 525, 463, 19, 128, 109, 517, 483, 54, 123, 466, 335, 587, 301, 40, 552, 334, 343, 285, 336, 46, 519, 547, 130, 489, 589, 161, 202, 158, 332, 222, 565, 131, 250, 94, 277, 226, 450, 357, 487, 424, 527, 535, 60, 144, 500, 247, 185, 467, 597, 132, 567, 532, 182, 578, 61, 142, 279, 505, 289, 529, 455, 355, 63, 25, 549, 546, 550, 180, 563, 317, 190, 239, 293, 253, 542, 495, 572, 66, 453, 175, 207
	Validation	35, 119, 55, 88, 540, 300, 6, 267, 93, 259, 156, 379, 588, 284, 39, 307, 445, 430, 0, 492, 431, 62, 235, 397, 299, 283, 349, 23, 221, 147, 281, 140, 83, 233, 10, 251, 488, 526, 318, 391, 90, 7, 303, 100, 263, 188, 376, 45, 356, 178, 586, 509, 290, 9, 435, 324, 471, 291, 388, 154, 139, 32, 436, 385, 374, 548, 260, 496, 504, 77, 363, 417, 377, 203, 282, 577, 557, 337, 564, 294, 373, 81, 29, 200, 58, 545, 78, 399, 514, 2, 102, 384, 24, 171, 327, 484, 321, 358, 465, 351, 169, 153, 56, 347, 275, 14, 246, 469, 197, 214, 254, 440, 257, 434, 266, 95, 583, 211, 204, 101, 138
	Test	460, 401, 348, 149, 292, 228, 244, 166, 107, 236, 3, 273, 143, 528, 43, 258, 274, 51, 162, 70, 230, 313, 113, 485, 104, 74, 209, 242, 304, 353, 271, 245, 111, 270, 378, 441, 114, 205, 136, 36, 493, 479, 433, 13, 331, 409, 213, 594, 183, 429, 65, 126, 49, 64, 302, 425, 172, 187, 173, 508, 99, 382, 575, 262, 478, 82, 115, 486, 255, 407, 189, 248, 217, 346, 199, 276, 191, 598, 194, 584, 438, 231, 48, 603, 553, 72, 521, 459, 206, 11, 44, 368, 223, 415, 296, 165, 405, 418, 326, 570, 298, 1, 125, 218, 342, 192, 141, 413, 398, 420, 375, 157, 159, 227, 473, 339, 26, 380, 395, 561, 367

Table 11: Taskset partitions for tiered-ImageNet. (continued)

Setting	Taskset	Classes
D = 0.64	Train	14, 582, 59, 559, 181, 209, 323, 506, 464, 562, 76, 524, 310, 316, 352, 65, 254, 216, 29, 516, 89, 298, 520, 177, 235, 101, 360, 274, 427, 344, 283, 230, 138, 302, 509, 100, 147, 246, 231, 227, 457, 217, 229, 187, 37, 232, 173, 264, 127, 27, 99, 322, 238, 601, 371, 168, 472, 103, 437, 287, 225, 160, 53, 164, 574, 473, 518, 479, 73, 604, 52, 591, 77, 599, 170, 359, 135, 263, 115, 513, 241, 454, 327, 501, 275, 330, 502, 576, 350, 98, 272, 538, 406, 558, 17, 198, 42, 475, 195, 432, 108, 21, 30, 153, 426, 151, 311, 339, 47, 499, 22, 114, 534, 449, 67, 333, 592, 105, 548, 560, 593, 523, 120, 556, 533, 461, 436, 381, 262, 86, 122, 428, 96, 503, 462, 353, 197, 402, 392, 607, 374, 291, 544, 57, 458, 444, 551, 296, 331, 117, 510, 102, 470, 541, 602, 145, 186, 585, 466, 320, 571, 118, 554, 606, 471, 555, 490, 134, 5, 208, 566, 319, 443, 226, 373, 537, 587, 387, 306, 600, 477, 308, 212, 31, 404, 564, 596, 326, 176, 44, 269, 224, 312, 605, 476, 38, 439, 400, 494, 278, 91, 268, 146, 552, 480, 590, 578, 196, 345, 286, 4, 125, 92, 261, 434, 41, 192, 28, 565, 159, 40, 243, 112, 97, 211, 50, 440, 71, 386, 280, 412, 517, 33, 569, 498, 500, 332, 366, 581, 358, 110, 394, 121, 19, 116, 297, 519, 511, 309, 8, 338, 474, 129, 169, 295, 408, 79, 487, 357, 343, 536, 185, 219, 403, 305, 354, 68, 491, 535, 579, 512, 152, 505, 525, 252, 315, 184, 109, 563, 543, 515, 240, 361, 463, 595, 546, 550, 130, 522, 456, 128, 539, 54, 396, 372, 334, 179, 106, 568, 148, 336, 15, 450, 567, 329, 547, 335, 419, 202, 132, 589, 123, 46, 448, 542, 451, 201, 150, 182, 370, 549, 131, 161, 142, 155, 279, 580, 317, 63, 174, 163, 222, 285, 66, 250, 424, 190, 572, 61, 453, 94, 239, 277, 573, 60, 489, 25, 293, 355, 253, 289, 495, 301, 158, 455, 247, 180, 483, 467, 144, 527, 597, 532, 175, 529, 207
	Validation	348, 156, 3, 378, 259, 356, 379, 162, 313, 13, 588, 74, 236, 324, 304, 55, 166, 303, 445, 35, 460, 9, 214, 508, 486, 405, 104, 242, 351, 478, 276, 376, 149, 488, 496, 594, 409, 459, 398, 603, 465, 140, 526, 20, 281, 299, 39, 48, 136, 492, 215, 570, 255, 233, 493, 540, 341, 204, 365, 364, 414, 88, 325, 62, 411, 270, 416, 415, 388, 75, 257, 83, 346, 69, 133, 16, 249, 413, 248, 199, 137, 194, 507, 294, 7, 258, 553, 188, 2, 531, 410, 271, 1, 342, 446, 203, 256, 221, 431, 126, 172, 34, 363, 307, 395, 265, 468, 218, 328, 273, 24, 80, 390, 481, 266, 442, 87, 139, 530, 447, 141
	Test	228, 6, 401, 300, 51, 93, 429, 23, 385, 349, 143, 441, 245, 64, 70, 586, 377, 78, 213, 545, 205, 528, 430, 72, 45, 282, 18, 485, 11, 82, 384, 81, 56, 84, 178, 119, 113, 314, 575, 423, 418, 375, 368, 407, 292, 267, 340, 598, 90, 49, 417, 584, 399, 244, 438, 191, 165, 157, 223, 284, 124, 43, 433, 183, 557, 521, 32, 154, 504, 260, 318, 382, 107, 362, 234, 383, 367, 422, 435, 171, 12, 210, 10, 189, 111, 452, 237, 420, 290, 380, 514, 484, 193, 36, 425, 206, 220, 85, 561, 421, 347, 167, 393, 58, 497, 0, 583, 251, 577, 26, 200, 389, 469, 482, 397, 288, 95, 321, 369, 391, 337
D = 0.96	Train	600, 509, 217, 138, 225, 220, 481, 164, 341, 565, 69, 359, 135, 602, 430, 409, 193, 550, 435, 103, 380, 498, 104, 390, 265, 479, 215, 392, 17, 488, 375, 268, 368, 535, 505, 461, 99, 101, 198, 254, 147, 287, 476, 546, 494, 236, 556, 592, 276, 100, 145, 281, 31, 339, 153, 487, 146, 14, 519, 58, 496, 477, 563, 230, 517, 9, 433, 115, 203, 28, 24, 492, 562, 555, 141, 425, 311, 274, 523, 57, 534, 591, 302, 369, 574, 291, 485, 21, 235, 181, 208, 478, 186, 80, 395, 273, 475, 130, 22, 117, 283, 333, 264, 32, 490, 263, 538, 551, 120, 132, 548, 458, 110, 436, 212, 411, 266, 312, 590, 559, 352, 197, 374, 278, 102, 231, 486, 321, 189, 581, 322, 387, 406, 50, 363, 389, 553, 542, 41, 344, 575, 508, 308, 447, 91, 347, 330, 114, 306, 182, 373, 5, 66, 499, 59, 280, 501, 474, 288, 323, 1, 560, 463, 86, 172, 350, 338, 176, 320, 439, 142, 317, 468, 112, 450, 105, 319, 427, 393, 549, 262, 432, 19, 27, 598, 40, 491, 71, 331, 256, 129, 402, 453, 440, 168, 219, 584, 564, 10, 53, 159, 525, 8, 237, 44, 537, 326, 134, 92, 196, 589, 242, 122, 353, 547, 296, 68, 342, 394, 567, 209, 202, 603, 309, 434, 211, 480, 426, 536, 345, 577, 337, 299, 570, 96, 109, 121, 272, 444, 190, 47, 471, 305, 240, 192, 261, 297, 185, 428, 29, 125, 200, 569, 403, 184, 286, 152, 42, 572, 243, 127, 354, 252, 54, 544, 221, 33, 381, 148, 511, 79, 334, 400, 539, 497, 327, 131, 106, 229, 150, 456, 269, 279, 579, 358, 372, 336, 595, 451, 412, 232, 443, 543, 522, 179, 473, 224, 295, 52, 163, 361, 169, 512, 123, 201, 128, 568, 15, 515, 404, 396, 239, 580, 366, 4, 357, 495, 329, 472, 187, 173, 335, 293, 222, 448, 253, 386, 46, 77, 174, 155, 573, 370, 275, 61, 25, 161, 408, 158, 97, 285, 489, 116, 315, 277, 250, 467, 94, 355, 301, 455, 247, 424, 60, 180, 289, 144, 419, 483, 527, 175, 63, 597, 532, 529, 207
	Validation	156, 259, 124, 23, 133, 20, 162, 89, 13, 245, 136, 356, 199, 45, 526, 531, 378, 191, 165, 514, 594, 82, 429, 84, 223, 282, 55, 95, 226, 314, 459, 248, 524, 241, 154, 318, 414, 34, 157, 260, 518, 171, 2, 26, 601, 292, 39, 582, 558, 90, 6, 36, 452, 464, 328, 449, 457, 85, 170, 284, 398, 37, 139, 216, 521, 12, 418, 56, 604, 111, 503, 38, 271, 73, 533, 376, 183, 270, 249, 587, 251, 137, 599, 607, 118, 462, 316, 332, 346, 540, 437, 151, 107, 500, 246, 143, 420, 557, 585, 160, 605, 484, 520, 98, 552, 294, 206, 576, 30, 233, 383, 438, 367, 513, 482, 258, 442, 388, 195, 343, 566
	Test	348, 228, 3, 93, 325, 545, 78, 213, 324, 465, 300, 303, 64, 11, 166, 140, 81, 51, 205, 588, 493, 401, 18, 460, 238, 214, 530, 35, 445, 177, 74, 583, 586, 385, 72, 507, 504, 48, 83, 469, 304, 516, 149, 188, 340, 113, 257, 119, 210, 49, 167, 466, 593, 415, 421, 365, 267, 362, 290, 416, 405, 204, 76, 7, 578, 441, 234, 255, 310, 218, 351, 87, 194, 16, 606, 423, 454, 244, 62, 379, 596, 399, 377, 384, 422, 88, 227, 502, 571, 391, 70, 431, 126, 554, 407, 528, 307, 413, 541, 364, 446, 43, 397, 108, 178, 0, 506, 75, 298, 67, 410, 360, 561, 65, 371, 510, 313, 417, 470, 349, 382